Hindawi
Archaea
Volume 2020, Article ID 8891543, 9 pages
https://doi.org/10.1155/2020/8891543

Research Article

Biosorption Mechanism of Aqueous Pb^{2+}, Cd^{2+}, and Ni^{2+} Ions on Extracellular Polymeric Substances (EPS)

Di Cui,[1] **Chong Tan**,[1] **Hongna Deng**,[1] **Xunxue Gu**,[1] **Shanshan Pi**,[2] **Ting Chen**,[2] **Lu Zhou**,[2] **and Ang Li**[2]

[1]*Pharmaceutical Engineering Technology Research Center, Harbin University of Commerce, Harbin 150076, China*
[2]*State Key Laboratory of Urban Water Resource and Environment, School of Environment, Harbin Institute of Technology, Harbin 150090, China*

Correspondence should be addressed to Di Cui; jscz_dd@hotmail.com and Ang Li; ang.li.harbin@gmail.com

Received 21 May 2020; Revised 8 June 2020; Accepted 9 June 2020; Published 24 June 2020

Academic Editor: Jin Li

Heavy metal pollution has been a focus with increasing attention, especially Pb^{2+}, Cd^{2+}, and Ni^{2+} in an aqueous environment. The adsorption capacity and mechanism of extracellular polymeric substances (EPS) from *Agrobacterium tumefaciens* F2 for three heavy metals were investigated in this study. The adsorption efficiency of 94.67%, 94.41%, and 77.95% were achieved for Pb^{2+}, Cd^{2+}, and Ni^{2+} adsorption on EPS, respectively. The experimental data of adsorption could be well fitted by Langmuir, Freundlich, Dubinin–Radushkevich isotherm models, and pseudo-second-order kinetic model. Model parameters analysis demonstrated the great adsorption efficiency of EPS, especially for Pb^{2+}, and chemisorption was the rate-limiting step during the adsorption process. The functional groups of C=O of carboxyl and C-O-C from sugar derivatives in EPS played the major role in the adsorption process judged by FTIR. In addition, 3D-EEM spectra indicated that tyrosine also assisted EPS adsorption for three heavy metals. But EPS from strain F2 used the almost identical adsorption mechanism for three kinds of divalent ions of heavy metals, so the adsorption efficiency difference of Pb^{2+}, Cd^{2+}, and Ni^{2+} on EPS could be correlated to the inherent characteristics of each heavy metal. This study gave the evidence that EPS has a great application potential as a bioadsorbent in the treatment of heavy metals pollution.

1. Introduction

Heavy metal pollution mainly comes from papermaking, smelting, electroplating, and other industrial wastewater and the overuse of pesticide and fertilizer [1]. Heavy metal pollutants are potentially harmful to the environment and human health, and they are not easily degraded by microorganisms in water. People intake heavy metal-contaminated water or food over an extended period, then they will suffer from various diseases or even cancer, such as anemia, bone pain, and chronic respiratory diseases for a long-term exposure to lead, cadmium, and nickel. In general, contaminated water often contains more than one heavy metal, such as industrial effluents, municipal wastewater, and industrial wastewater [2–4]. Therefore, exploring effective methods for controlling heavy metal pollution and improving the water environment, especially for lead, cadmium, and nickel, are necessary.

At present, the most commonly used treatment techniques for heavy metal pollution include chemical precipitation, ion exchange, adsorption, membrane separation, oxidation reduction, and electrochemical [5–22]. Among these methods, adsorption is preferred for its simplicity, efficiency, flexibility in design, low waste production, and environmental-friendly characteristics for certain biosorbents [23]. Recently, microbial extracellular polymeric substances (EPS) have become a popular research topic in the effective treatment of heavy metal pollution due to its safety, efficiency, low energy consumption, and simple operation [24–30].

EPS produced by *Agrobacterium tumefaciens* F2 is a complex compound with high molecular weight and used

Table 1: Thermodynamic and kinetics models of heavy metals adsorption on EPS.

Models	Formula	Model parameters
Langmuir adsorption isothermal model	$q_e = q_m bC_e/1 + \mathrm{b}C_e$	C_e——the initial concentration of heavy metals ($\mathrm{mg\,L^{-1}}$) q_e——the unit adsorption capacity when the initial concentration is Ce ($\mathrm{mg\,g^{-1}}$) q_m——maximum unit adsorption capacity ($\mathrm{mg\,g^{-1}}$) b——Langmuir adsorption equilibrium constant ($\mathrm{L\,mg^{-1}}$)
Freundlich adsorption isothermal model	$q_e = K_F C_e^{1/n}$	K_F——adsorption capacity ($\mathrm{mg\,g^{-1}}$) $1/n$——Freundlich adsorption capacity
Dubinin–Radushkevich adsorption isothermal model	$q_e = q_m \exp\left(-k\varepsilon^2\right)$ $\varepsilon = RT \ln\left(1 + (1/C_e)\right)$	q_e——equilibrium adsorption capacity ($\mathrm{mg\,g^{-1}}$) q_m——maximum unit adsorption capacity ($\mathrm{mg\,g^{-1}}$) k——constant related to adsorption capacity ($\mathrm{mol^2/kJ^2}$) R——ideal gas constant ($8.314\,\mathrm{J\,mol^{-1}\,K^{-1}}$) T——thermodynamic temperature C_e——initial concentration of contaminants ($\mathrm{mg\,L^{-1}}$) Average adsorption energy $E = (2\,\mathrm{k})^{-0.5}$
Pseudo-first order kinetics model	$\log(q_t - q_e) = \log q_e - (k_1/2.303)t$	t——adsorption time (min); q_t——unit adsorption capacity after t min ($\mathrm{mg\,g^{-1}}$); q_e——the maximum unit adsorption capacity ($\mathrm{mg\,g^{-1}}$); k_1——pseudo-first-order reaction rate constant
Pseudo-second order kinetics model	$t/q_t = \left(1/k_2 q_e^2\right) + (1/q_e)t$	k_2——pseudo-second-order reaction rate constant

to adsorb Pb^{2+}, Cd^{2+}, and Ni^{2+} pollutants in this study. Our previous researches focused on heavy metals or antibiotics adsorbed by bioflocculant MFX, which is one kind of EPS extracted from *Klebsiella* sp. J1 [31–38]. The results showed the great potential of EPS as water treatment materials and guided our subsequent studies. However, the main components of EPS produced by strain F2 are polysaccharide, which is different from the protein as the main component in bioflocculant MFX produced by strain J1. It was still unknown for the application potential of EPS produced by strain F2. Thus, it was used to adsorb heavy metal contaminants, and the adsorption mechanisms were systematically investigated via qualitative and quantitative analyses, thereby providing a new available bioadsorbent in water treatment.

2. Experimental Section

2.1. Strains and Reagents. Agrobacterium tumefaciens F2 is isolated by our group and now deposited in the China Common Microbial Culture Collection (CGMCC No. 10131). Lead nitrate, cadmium chloride, and nickel nitrate were purchased from Sigma-Aldrich, St Louis, MO, USA. Medium components were purchased from the Sinopharm Chemical Reagent Co., Ltd., Shanghai, China. Ultrapure water for all experiments was prepared with the Milli-Q system. All chemicals were analytical grade.

2.2. EPS Preparation. Strain F2 was applied to prepare EPS by the fermentation culture. The fermentation medium was composed of the following ingredients (g/L): glucose10, K_2HPO_4 5, KH_2PO_4 2, NaCl 0.1, $MgSO_4 \bullet 7H_2O$ 0.2, yeast extract 0.5, and urea 0.5 adjusted at pH 7.2-7.5. Strain F2 was precultured in the fermentation medium to obtain the seed liquid, which was then inoculated into the fermentation medium with 5% carried by a sterilized fermentor. The relevant culture parameters were set at 30°C, 150 rpm for 24 h with $2.5\,\mathrm{L\,min^{-1}}$. Then, the final fermentation liquid was centrifuged to eliminate the bacteria, and the precooling ethanol was added into the residual supernatant to collect white flocs and then dialyzed for 24 h. The flocs were freeze-dried by vacuum to obtain the dry powder of EPS and dissolved into ultrapure water before use.

2.3. Batch Adsorption Experiments. The stock solutions ($100\,\mathrm{mg\,L^{-1}}$) of Pb^{2+}, Cd^{2+}, and Ni^{2+} were prepared by dissolving lead nitrate, cadmium chloride, and nickel nitrate in ultrapure water. Working solutions were obtained by appropriate dilution of the stock solutions with ultrapure water and pH adjustment using $1\,\mathrm{mol\,L^{-1}}$ HNO_3 or NaOH. In each batch adsorption experiment, 0.2, 0.7, and $0.8\,\mathrm{g\,L^{-1}}$ adsorbents were added into 20 mL of Pb^{2+}, Cd^{2+}, and Ni^{2+} aqueous solution ($20\,\mathrm{mg\,L^{-1}}$, pH 6.0) and stirred for 0–70 min at 30°C. After adsorption, the concentrations of initial and residual ions in the aqueous solution were then measured by inductively coupled plasma optical emission spectrometry (ICP-OES; Optima 5300 DV, PE, USA) with the detection limit of $10\,\mu\mathrm{g\,L^{-1}}$. All samples were filtered by $0.45\,\mu$m cellulose acetate fiber before measurement. The adsorption efficiency (η) and the adsorption capacity (q_e) of Pb^{2+}, Cd^{2+}, and Ni^{2+} on EPS were calculated as follows:

$$qe = \frac{(C0 - Ce)\,V}{M}, \tag{1}$$

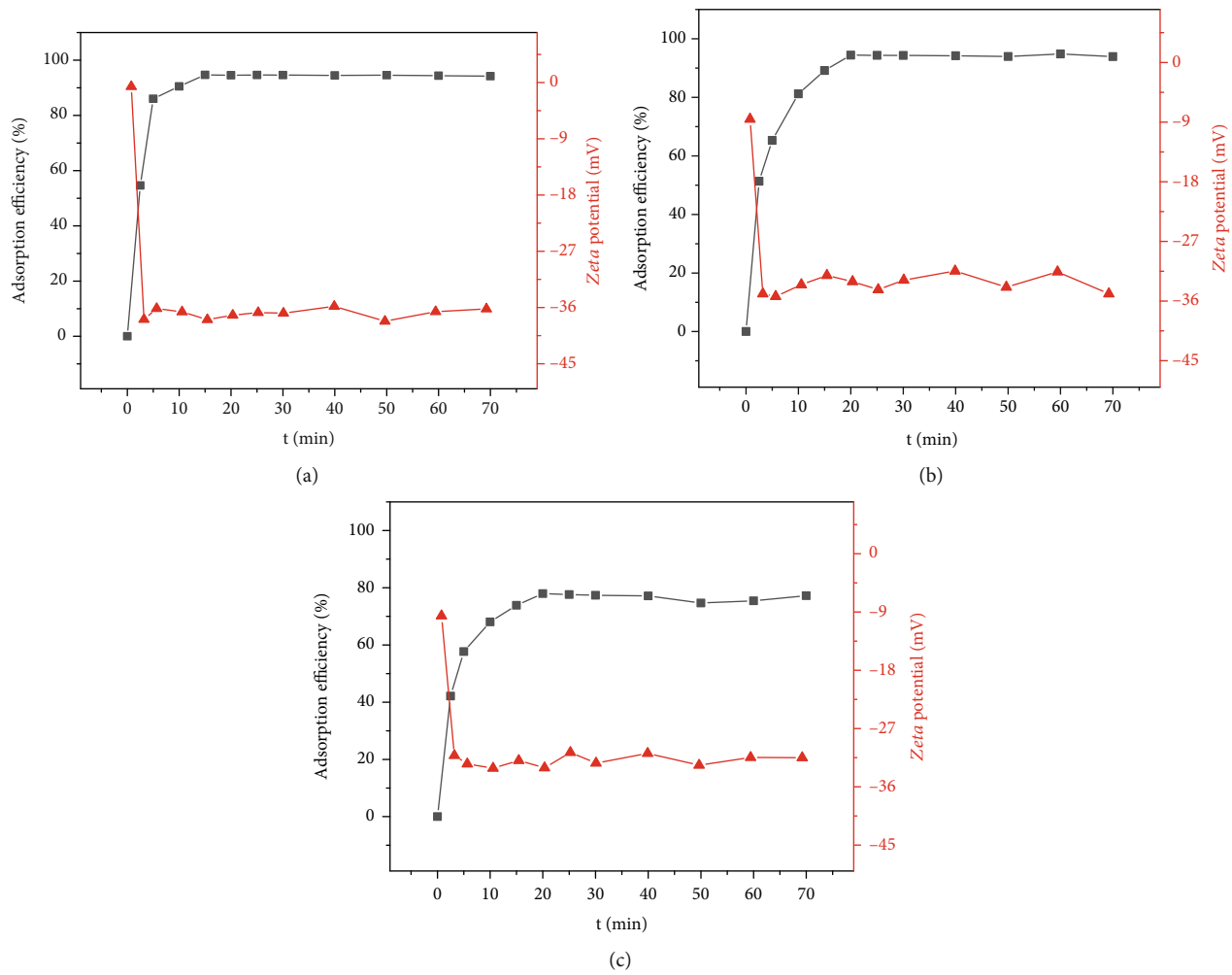

Figure 1: Adsorption efficiency and *Zeta* potential of Pb^{2+} (a), Cd^{2+} (b), and Ni^{2+} (c) adsorption on EPS.

$$\eta = \frac{(C0 - Ce)}{C0} \times 100\%, \quad (2)$$

where C_0 and C_e are the initial and equilibrium concentrations of heavy metal ion, respectively (mg L^{-1}), V is the solution volume (L), and M is the used amount of EPS (g). The average values were recorded with standard deviations within ±1.3%, and some error bars are not shown due to the magnitude being smaller than that of the symbols used to plot the graphs.

2.4. Adsorption Isotherms and Kinetics. Langmuir, Freundlich, and Dubinin–Radushkevich isotherm models were used to determine the sorption equilibrium at 20°C, 30°C, and 40°C, respectively. To investigate the adsorption isotherm, the initial concentration of heavy metal ions was ranged at 5–50 mg L^{-1}, and other conditions were consistent with the abovementioned batch adsorption experiments. For sorption kinetic experiment of heavy metal ions on EPS, the experimental data were analyzed using pseudo-first-order and pseudo-second-order kinetic models. The sorption time was during 2.5–70 min, and other parameters were the same with the abovementioned batch adsorption experiments. All models and key parameters are shown in Table 1.

2.5. Characterization of Adsorption Mechanism. The adsorption mechanism of heavy metal ions on EPS and characteristics before and after adsorption was analyzed using Fourier-transform infrared spectroscopy (FTIR), *Zeta* potential analysis, and three-dimensional fluorescence spectrophotometry (3D-EEM) to examine the interactions between EPS and Pb^{2+}, Cd^{2+}, and Ni^{2+}, respectively. EPS loading Pb^{2+}, Cd^{2+}, and Ni^{2+} samples under the optimal experimental conditions were collected and then rinsed to remove free heavy metal ions using ultrapure water. EPS (before and after Pb^{2+}, Cd^{2+}, and Ni^{2+} loading) were processed by vacuum freeze-drying. The spectra in the range of 400–4000 cm^{-1} were recorded via an FTIR spectrometer using the KBr disc technique. The *Zeta* potential of the system in the entire process was measured with zeta meter equipment. 3D-EEM was applied to study the variation of active ingredients before and after adsorption via a three-dimensional fluorescence spectrometer (FP6500, JASCO, Japan). Scanning parameters were set as the emission spectra of 220–450 nm at 1 nm increment by varying the excitation wavelength of 220–650 nm at

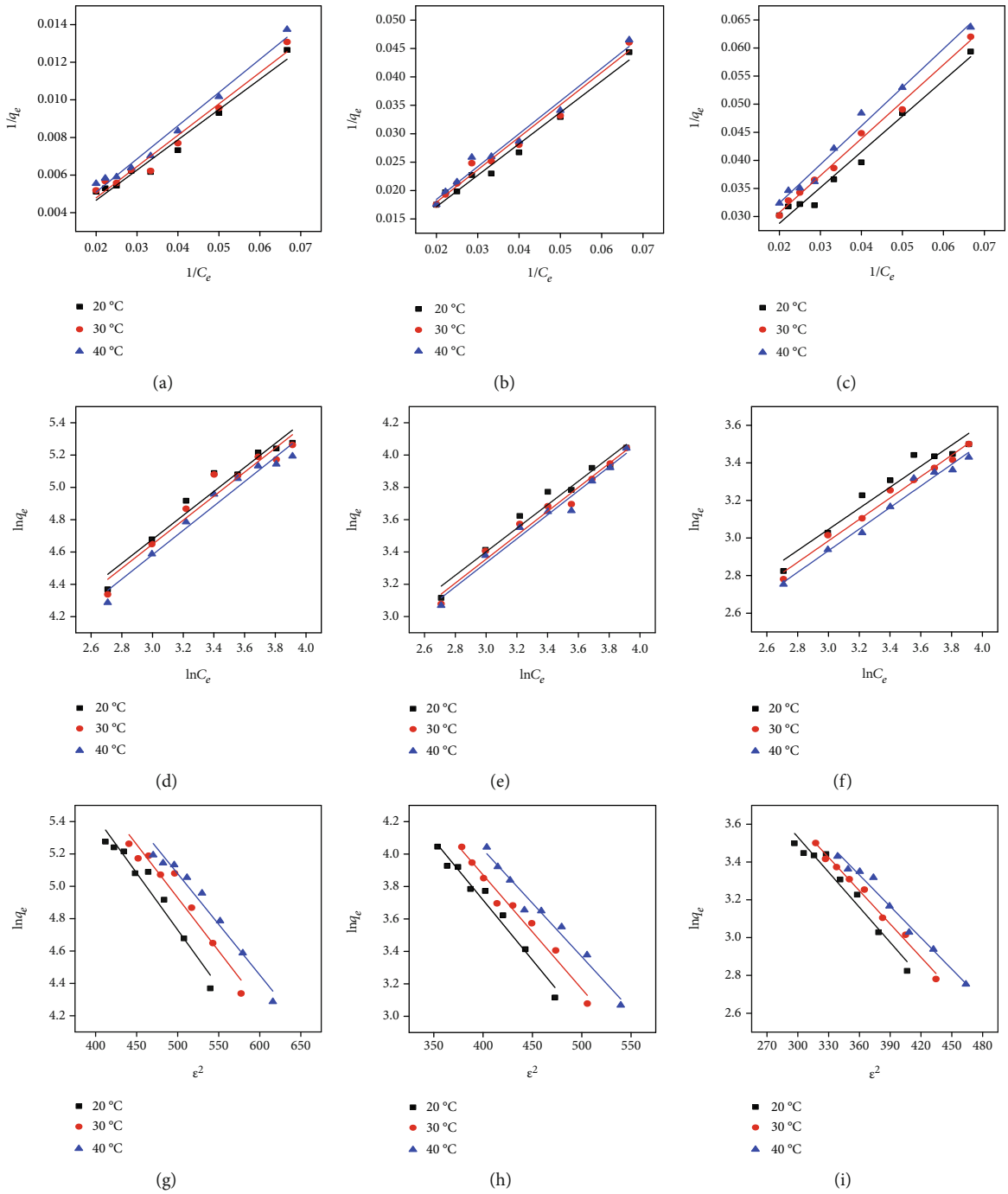

Figure 2: Continued.

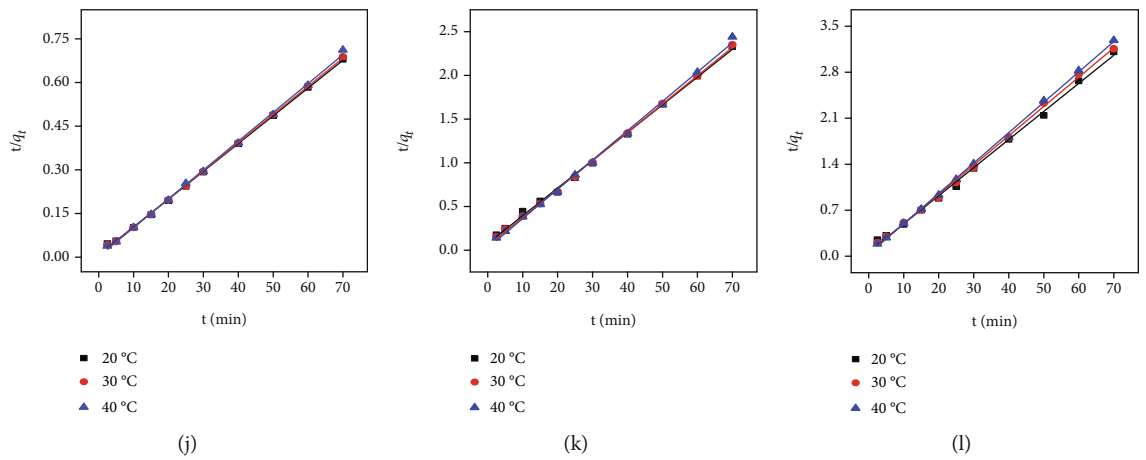

Figure 2: Langmuir (a–c), Freundlich (d–f), Dubinin–Radushkevich (g–i) isotherms, and pseudo-second-order kinetics (j–l) model of Pb^{2+}, Cd^{2+}, and Ni^{2+}adsorption on EPS.

5 nm increment. A blank solution (Milli-Q water) was subtracted from the sample.

3. Results and Discussion

3.1. Adsorption Efficiency of Heavy Metals on EPS. Figure 1 shows the adsorption efficiency and *Zeta* potential of metal ions on EPS at different adsorption time. The adsorption efficiency increased rapidly in the initial 5 min and increased gradually until adsorption saturation at almost 20 min with the highest adsorption efficiency of 94.67%, 94.41%, and 77.95% for Pb^{2+}, Cd^{2+}, and Ni^{2+} on EPS. Thus, EPS exhibited superior adsorption efficiency for target pollutants, especially Pb^{2+} and Cd^{2+}. However, the adsorption efficiency for Ni^{2+} on EPS is clearly not as ideal as Pb^{2+} and Cd^{2+}, so the further adsorption mechanism is still needed to explain the adsorption difference. *Zeta* potential analysis was used to analyze the stability of adsorption reaction along with different time before and after Pb^{2+}, Cd^{2+}, and Ni^{2+} adsorption on EPS. As seen in Figure 1(b), the *Zeta* potentials of reaction system rapidly decreased after adding EPS into Pb^{2+}, Cd^{2+}, and Ni^{2+} and reached stable at -37.90, -34.9, and -31.2 mV, respectively. Subsequently, the *Zeta* potential remained stable along with the increased adsorption efficiency, thus indicating that the whole adsorption reaction process is stable. Negatively charged EPS was favorable for its adsorption for positively charged heavy metals, so it exhibited the superior adsorption efficiency for Pb^{2+}, Cd^{2+}, and Ni^{2+}.

3.2. Isotherm Models

3.2.1. Langmuir Adsorption Isotherm Model. The fitting results of the Langmuir adsorption isotherms of Pb^{2+}, Cd^{2+}, and Ni^{2+} on EPS at 20°C, 30°C, and 40°C are shown in Figures 2(a)–2(c). The results showed that the R^2 are all greater than 0.90, indicating that Pb^{2+}, Cd^{2+}, and Ni^{2+} adsorption on EPS could be fitted well by Langmuir adsorption isotherm models. The data for the adsorption process of Pb^{2+}, Cd^{2+}, and Ni^{2+} on EPS satisfactorily fitted to the Langmuir model in an aquatic system with $R^2 > 0.90$, indicating that monolayer adsorption could exist [31]. The model parameters are shown in Table 2, in which q_m gradually decreases and b increases with the increased temperature, indicating the exothermic nature of the adsorption process.

Table 2: Parameters of Langmuir adsorption isotherms.

Heavy metals	Temperature (°C)	q_m (mg g^{-1})	b (L mg^{-1}) × 10^{-3}	R^2
Pb^{2+}	20	714.29	8.71	0.97
	30	666.67	9.01	0.97
	40	625.00	9.07	0.98
Cd^{2+}	20	104.17	20.16	0.96
	30	97.09	21.03	0.96
	40	92.59	21.80	0.96
Ni^{2+}	20	51.28	34.20	0.96
	30	48.08	35.48	0.94
	40	45.05	36.53	0.97

Table 3: Parameters of Freundlich adsorption isotherms.

Heavy metals	Temperature (°C)	K_F (mg g^{-1})	n	R^2
Pb^{2+}	20	11.63	1.3484	0.95
	30	11.22	1.3452	0.94
	40	10.18	1.3259	0.97
Cd^{2+}	20	5.05	1.6739	0.93
	30	4.68	1.6464	0.94
	40	4.57	1.6447	0.95
Ni^{2+}	20	4.69	2.0080	0.94
	30	4.47	2.0076	0.93
	40	4.25	2.0072	0.97

3.2.2. Freundlich Adsorption Isotherm Model. The fitting results of the Freundlich isotherm model are shown in Figures 2(d)–2(f), and the model parameters are presented in Table 3. The results suggested that adsorption of Pb^{2+},

Table 4: Parameters of Dubinin–Radushkevich model.

Heavy metals	Temperature (°C)	E (kJ mol^{-1})	R^2
Pb^{2+}	20	8.45	0.96
	30	8.70	0.95
	40	8.91	0.97
Cd^{2+}	20	9.05	0.93
	30	9.28	0.95
	40	9.62	0.95
Ni^{2+}	20	9.53	0.95
	30	9.90	0.93
	40	10.21	0.97

Table 5: Parameters of pseudo-second-order kinetics model.

Heavy metals	Temperature (°C)	q_m (mg g^{-1})	k_2 (min^{-1}) × 10^{-2}	R^2
Pb^{2+}	20	105.26	1.04	0.99
	30	103.09	1.57	0.99
	40	101.01	3.77	0.99
Cd^{2+}	20	31.55	1.33	0.99
	30	30.86	2.09	0.99
	40	29.85	4.40	0.99
Ni^{2+}	20	23.42	2.74	0.99
	30	22.42	4.00	0.99
	40	21.65	6.45	0.99

Cd^{2+}, and Ni^{2+} on EPS is also consistent with the Freundlich isotherm model with $R^2 > 0.90$. With the gradual increase of temperature, the gradually decreased K_F of Pb^{2+}, Cd^{2+}, and Ni^{2+} adsorption on EPS indicated that the adsorption reaction is exothermic [39]. $n > 1$ indicated the good adsorption capacity of Pb^{2+}, Cd^{2+}, and Ni^{2+} on EPS [31, 37].

3.2.3. Dubinin–Radushkevich Adsorption Isotherm Model. The model is used to judge whether the adsorption process is completed by a physical or chemical reaction [40]. The model parameters of Dubinin–Radushkevich can be used to explain the adsorption process with $R^2 > 0.90$. The fitting results of Dubinin–Radushkevich models and parameters at 20°C, 30°C, and 40°C are presented in Figures 2(g)–2(i) and Table 4, respectively. Based on the Dubinin–Radushkevich model, the physical adsorption is resulted from Van der Waals forces judged by that E value was lower than 8 kJ mol^{-1}, whereas the chemical adsorption usually involves ion exchange judged by that the E value was 8–16 kJ mol^{-1} [41]. E values of Pb^{2+}, Cd^{2+}, and Ni^{2+} adsorption on EPS are between 8 kJ mol^{-1} and 16 kJ mol^{-1}, respectively, indicating that the adsorption process is mainly completed by the chemical adsorption. The above analysis showed that the adsorption process of Pb^{2+}, Cd^{2+}, and Ni^{2+} on EPS could be well fitted by the Langmuir, Freundlich, and Dubinin–Radushkevich isotherm models ($R^2 > 0.90$), indicating the complex adsorption process involved in multiple adsorption mechanism, especially chemical adsorption related to ion exchange.

3.3. Kinetic Models. The pseudo-first- and second-order kinetic models were applied to fit the data for adsorption behavior. However, the pseudo-first-order dynamic model could not effectively fit the adsorption process with $R^2 <$ 0.80 (data not shown). The pseudo-second-order kinetic model is usually used to clarify the limiting step during the adsorption process. The model was used to analyze the adsorption process and mechanism via quantitative approaches in this study. The fitting results of the pseudo-second-order kinetics model are shown in Figures 2(j)–2(l), and the model parameters are presented in Table 5. $R^2 >$ 0.90 indicated that the adsorption process can be better fitted by the pseudo-second-order kinetic model. The results

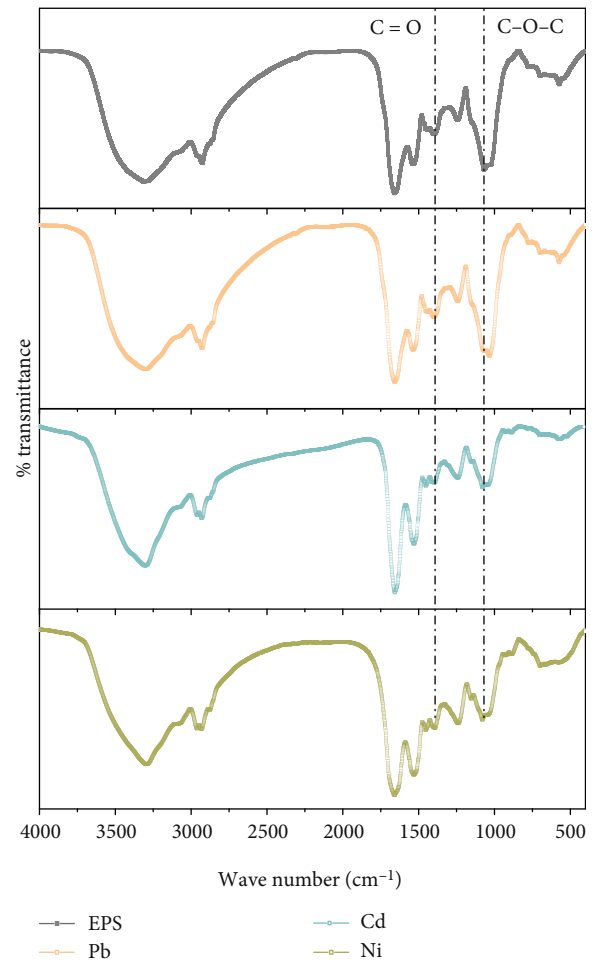

Figure 3: Functional group analysis of EPS before and after Pb^{2+}, Cd^{2+}, and Ni^{2+} adsorption.

showed that the chemical adsorption was the rate-limiting step during the adsorption process [24].

The apparent activation energy (Ea) is calculated from the reaction rate k based on the Arrhenius formula in the pseudo-second-order kinetics. The adsorption process is physical adsorption when the Ea is 5–40 kJ mol^{-1} and

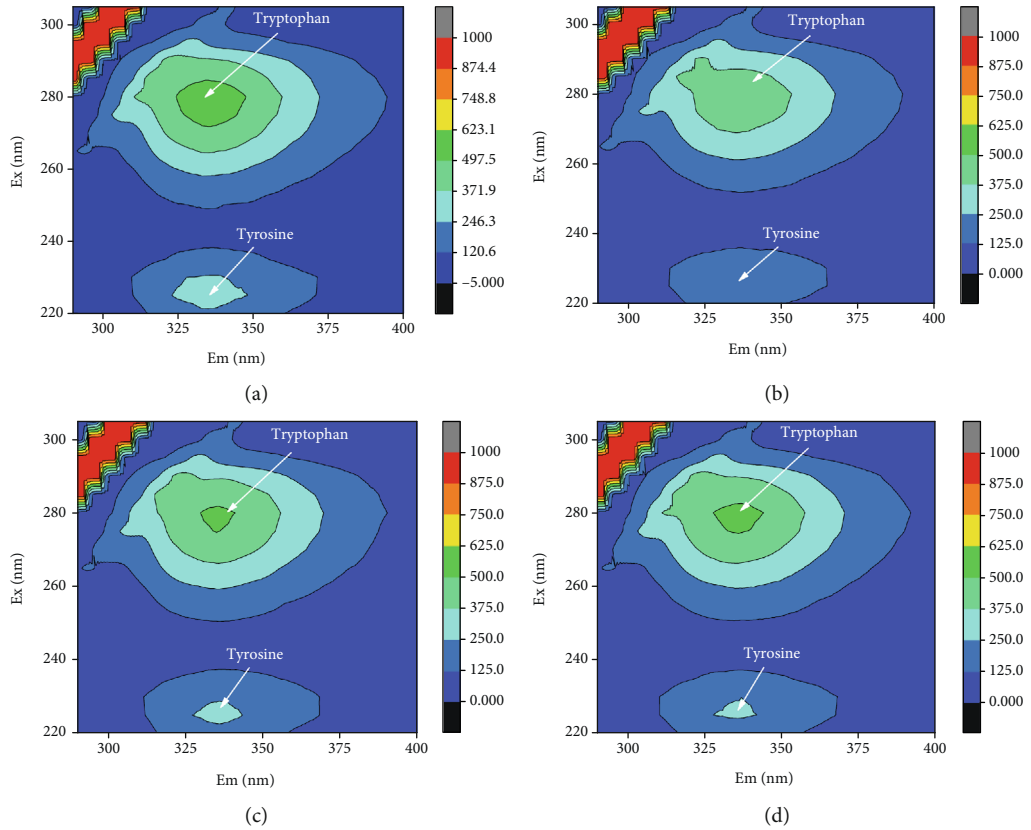

Figure 4: 3D-EEM spectrum of EPS (a) before adsorption, and after adsorption of (b) Pb^{2+}, (c) Cd^{2+}, (d) Ni^{2+}.

chemical adsorption when the *Ea* is 40–800 kJ mol^{-1} [32, 42]. The *Ea* values of Pb^{2+}, Cd^{2+}, and Ni^{2+} adsorption on EPS were 709.27, 660.44, and 472.23 kJ mol^{-1}, respectively, indicating a chemical adsorption process.

3.4. Adsorption Mechanism. Several studies have shown that the functional group is a key factor for contaminant adsorption on the EPS. The infrared spectra of EPS before and after adsorption of Pb^{2+}, Cd^{2+}, and Ni^{2+} are shown in Figure 3, and several peaks are observed, including O-H, C=O, N-H, C-N, C-O-C, and C-O in EPS [32, 33]. As shown in Figure 3, obvious changes of the peak intensity in C=O of carboxyl and C-O-C bands from sugar derivatives were observed after heavy metal adsorption. This finding might be explained by the polysaccharides as the main constituent in EPS played the key role during the adsorption process.

3D-EEM spectrum exhibited that $\lambda ex/\lambda em = (270 - 280)$ nm/$(325 - 335)$ nm and $\lambda ex/\lambda em = (225 - 235)$ nm/$(325 - 335)$ nm could represent aromatic amino acid tryptophan and tyrosine of protein-like substances [43]. Figure 4 showed that their fluorescence intensity weakened after EPS absorbing Pb^{2+}, Cd^{2+}, and Ni^{2+}, displaying different levels of quenching. The fluorescence intensity of tyrosine proteins in EPS showed relatively more obvious quenching after absorbing Pb^{2+}, Cd^{2+}, and Ni^{2+}. Results showed the tyrosine of protein-like substances in EPS also played a somewhat role in the adsorption for heavy metals. A possible explanation was that polysaccharide is the main component in EPS produced by strain F2 [44], while the low protein content in EPS resulted in the minor change during the adsorption of heavy metals.

In summary, EPS from strain F2 used the almost identical adsorption mechanism for three kinds of divalent ions of heavy metals. The adsorption efficiency difference of Pb^{2+}, Cd^{2+}, and Ni^{2+} on EPS could be correlated to the inherent characteristics of each heavy metals, which deserve an in-depth investigation via a quantitative structure–activity relationship (QSAR). The obvious changes in C=O of carboxyl and C-O-C bands from sugar derivatives via FTIR could support the viewpoint of that the polysaccharides as the main constituent in EPS played the key role during the adsorption process of Pb^{2+}, Cd^{2+}, and Ni^{2+} ions. In addition, the weak quenching changes in tyrosine of protein-like substances in EPS via 3D-EEM was also observed after absorbing heavy metals, which could indicate protein-like substances in EPS also assisted in heavy metals adsorption. At present, EPS has been reported to be used in the Sb(V) reduction and adsorption, which was enhanced through nZVI coating [45]. Therefore, we would consider applying EPS from strain F2 into the redox-adsorption of other substances, such as perchlorate and vanadate [46, 47], in the future work.

4. Conclusion

EPS from *Agrobacterium tumefaciens* F2 exhibited effective adsorption efficiency for Pb^{2+}, Cd^{2+}, and Ni^{2+}, especially for Pb^{2+}. But EPS from strain F2 used the almost identical adsorption mechanism for three kinds of divalent ions of

heavy metals, so the adsorption efficiency difference of Pb^{2+}, Cd^{2+}, and Ni^{2+} on EPS could be correlated to the inherent characteristics of each heavy metals. Thermodynamics and kinetics analysis displayed the exothermic nature of the adsorption process, the good adsorption capacity of adsorbents, and the key role of chemical adsorption. The adsorption mechanism demonstrated Pb^{2+}, Cd^{2+}, and Ni^{2+} adsorption on EPS was mainly attributed to the functional groups of the C=O of carboxyl and C-O-C from sugar derivatives. To some extent, amino acid protein-like substances in EPS also assisted in heavy metals adsorption. EPS from strain F2 as a bioadsorbent has great application potential in the treatment of heavy metal ions from contaminated aquatic systems.

Data Availability

Data can be available by contacting the corresponding author.

Conflicts of Interest

The authors declare no actual or potential competing financial interests.

Acknowledgments

This work was financially supported by the National Natural Science Foundation of China (51608154), the Foundation for Distinguished Young Talents in Higher Education of Heilongjiang, China (UNPYSCT-2017211), the Foundation for Distinguished Young Talents of Harbin University of Commerce, China (18XN026), and the PhD early development program of Harbin University of Commerce, China (2016BS15).

References

[1] A. Azimi, A. Azari, M. Rezakazemi, and M. Ansarpour, "Removal of heavy metals from industrial wastewaters: a review," *ChemBioEng Reviews*, vol. 4, no. 1, pp. 37–59, 2017.

[2] C. Wang, X. Hu, M. Chen, and Y. Wu, "Total concentrations and fractions of Cd, Cr, Pb, Cu, Ni and Zn in sewage sludge from municipal and industrial wastewater treatment plants," *Journal of Hazardous Materials*, vol. 119, no. 1-3, pp. 245–249, 2005.

[3] A. Demirbas, E. Pehlivan, F. Gode, T. Altun, and G. Arslan, "Adsorption of Cu(II), Zn(II), Ni(II), Pb(II), and Cd(II) from aqueous solution on Amberlite IR-120 synthetic resin," *Journal of Colloid and Interface Science*, vol. 282, no. 1, pp. 20–25, 2005.

[4] H. A. Aziz, M. N. Adlan, and K. S. Ariffin, "Heavy metals (Cd, Pb, Zn, Ni, Cu and Cr(III)) removal from water in Malaysia: post treatment by high quality limestone," *Bioresource Technology*, vol. 99, no. 6, pp. 1578–1583, 2008.

[5] M. Q. Jiang, X. Y. Jin, X. Q. Lu, and Z. L. Chen, "Adsorption of Pb(II), Cd(II), Ni(II) and Cu(II) onto natural kaolinite clay," *Desalination*, vol. 252, no. 1-3, pp. 33–39, 2010.

[6] S. Chatterjee and S. De, "Adsorptive removal of arsenic from groundwater using chemically treated iron ore slime incorporated mixed matrix hollow fiber membrane," *Separation and Purification Technology*, vol. 179, pp. 357–368, 2017.

[7] E. Padilla-Ortega, R. Leyva-Ramos, and J. V. Flores-Cano, "Binary adsorption of heavy metals from aqueous solution onto natural clays," *Chemical Engineering Journal*, vol. 225, pp. 535–546, 2013.

[8] A. Kongsuwan, P. Patnukao, and P. Pavasant, "Binary component sorption of Cu(II) and Pb(II) with activated carbon from Eucalyptus camaldulensis Dehn bark," *Journal of Industrial and Engineering Chemistry*, vol. 15, no. 4, pp. 465–470, 2009.

[9] Y. Chen, X. Wu, L. Lv et al., "Enhancing reducing ability of α-zein by fibrillation for synthesis of Au nanocrystals with continuous flow catalysis," *Journal of Colloid and Interface Science*, vol. 491, pp. 37–43, 2017.

[10] R. Mukherjee, P. Bhunia, and S. De, "Impact of graphene oxide on removal of heavy metals using mixed matrix membrane," *Chemical Engineering Journal*, vol. 292, pp. 284–297, 2016.

[11] K. Athanasiadis and B. Helmreich, "Influence of chemical conditioning on the ion exchange capacity and on kinetic of zinc uptake by clinoptilolite," *Water Research*, vol. 39, no. 8, pp. 1527–1532, 2005.

[12] B. Alyuz and S. Veli, "Kinetics and equilibrium studies for the removal of nickel and zinc from aqueous solutions by ion exchange resins," *Journal of Hazardous Materials*, vol. 167, no. 1-3, pp. 482–488, 2009.

[13] M. Kumar, R. Shevate, R. Hilke, and K. V. Peinemann, "Novel adsorptive ultrafiltration membranes derived from polyvinyltetrazole-co-polyacrylonitrile for Cu(II) ions removal," *Chemical Engineering Journal*, vol. 301, pp. 306–314, 2016.

[14] M. Mondal, M. Dutta, and S. De, "A novel ultrafiltration grade nickel iron oxide doped hollow fiber mixed matrix membrane: spinning, characterization and application in heavy metal removal," *Separation and Purification Technology*, vol. 188, pp. 155–166, 2017.

[15] B. A. Marinho, R. O. Cristóvão, R. Djellabi, J. M. Loureiro, R. A. R. Boaventura, and V. J. P. Vilar, "Photocatalytic reduction of Cr(VI) over TiO_2-coated cellulose acetate monolithic structures using solar light," *Applied Catalysis B: Environmental*, vol. 203, pp. 18–30, 2017.

[16] N. Abdullah, R. J. Gohari, N. Yusof et al., "Polysulfone/hydrous ferric oxide ultrafiltration mixed matrix membrane: preparation, characterization and its adsorptive removal of lead (II) from aqueous solution," *Chemical Engineering Journal*, vol. 289, pp. 28–37, 2016.

[17] Q. Chen, Z. Luo, C. Hills, G. Xue, and M. Tyrer, "Precipitation of heavy metals from wastewater using simulated flue gas: sequent additions of fly ash, lime and carbon dioxide," *Water Research*, vol. 43, no. 10, pp. 2605–2614, 2009.

[18] M. T. Alvarez, C. Crespo, and B. Mattiasson, "Precipitation of Zn(II), Cu(II) and Pb(II) at bench-scale using biogenic hydrogen sulfide from the utilization of volatile fatty acids," *Chemosphere*, vol. 66, no. 9, pp. 1677–1683, 2007.

[19] X. Li, H. Li, X. Xu, N. Guo, L. Yuan, and H. Yu, "Preparation of a reduced Graphene oxide @ stainless steel net electrode and its application of electrochemical removal Pb(II)," *Journal of the Electrochemical Society*, vol. 164, no. 4, pp. E71–E77, 2017.

[20] Q. Chang, M. Zhang, and J. Wang, "Removal of Cu^{2+} and turbidity from wastewater by mercaptoacetyl chitosan," *Journal of Hazardous Materials*, vol. 169, no. 1-3, pp. 621–625, 2009.

[21] W. Peng, H. Li, Y. Liu, and S. Song, "A review on heavy metal ions adsorption from water by graphene oxide and its composites," *Journal of Molecular Liquids*, vol. 230, pp. 496–504, 2017.

[22] S. Deng, P. Wang, G. Zhang, and Y. Dou, "Polyacrylonitrile-based fiber modified with thiosemicarbazide by microwave irradiation and its adsorption behavior for Cd(II) and Pb(II)," *Journal of Hazardous Materials*, vol. 307, pp. 64–72, 2016.

[23] D. P. Sounthararajah, P. Loganathan, J. Kandasamy, and S. Vigneswaran, "Adsorptive removal of heavy metals from water using sodium titanate nanofibres loaded onto GAC in fixed-bed columns," *Journal of Hazardous Materials*, vol. 287, pp. 306–316, 2015.

[24] J. Feng, Z. Yang, G. Zeng et al., "The adsorption behavior and mechanism investigation of Pb(II) removal by flocculation using microbial flocculant GA1," *Bioresource Technology*, vol. 148, pp. 414–421, 2013.

[25] L. Wei, Y. Li, D. R. Noguera et al., "Adsorption of Cu^{2+} and Zn^{2+} by extracellular polymeric substances (EPS) in different sludges: effect of EPS fractional polarity on binding mechanism," *Journal of Hazardous Materials*, vol. 321, pp. 473–483, 2017.

[26] M. Shahadat, T. T. Teng, M. Rafatullah, Z. A. Shaikh, T. R. Sreekrishnan, and S. W. Ali, "Bacterial bioflocculants: a review of recent advances and perspectives," *Chemical Engineering Journal*, vol. 328, pp. 1139–1152, 2017.

[27] N. Li, D. Wei, S. Wang et al., "Comparative study of the role of extracellular polymeric substances in biosorption of Ni(II) onto aerobic/anaerobic granular sludge," *Journal of Colloid and Interface Science*, vol. 490, pp. 754–761, 2017.

[28] J. Wang, Q. Li, M. M. Li, T. H. Chen, Y. F. Zhou, and Z. B. Yue, "Competitive adsorption of heavy metal by extracellular polymeric substances (EPS) extracted from sulfate reducing bacteria," *Bioresource Technology*, vol. 163, pp. 374–376, 2014.

[29] J. Guo and J. Yu, "Sorption characteristics and mechanisms of Pb(II) from aqueous solution by using bioflocculant MBFR10543," *Applied Microbiology and Biotechnology*, vol. 98, no. 14, pp. 6431–6441, 2014.

[30] P. Yan, J. S. Xia, Y. P. Chen et al., "Thermodynamics of binding interactions between extracellular polymeric substances and heavy metals by isothermal titration microcalorimetry," *Bioresource Technology*, vol. 232, pp. 354–363, 2017.

[31] A. Li, S. Pi, W. Wei, T. Chen, J. Yang, and F. Ma, "Adsorption behavior of tetracycline by extracellular polymeric substrates extracted from Klebsiella sp. J1," *Environmental Science and Pollution Research*, vol. 23, no. 24, pp. 25084–25092, 2016.

[32] W. Wei, Q. Wang, A. Li et al., "Biosorption of Pb (II) from aqueous solution by extracellular polymeric substances extracted from Klebsiella sp. J1: Adsorption behavior and mechanism assessment," *Scientific Reports*, vol. 6, no. 1, p. 31575, 2016.

[33] J. Yang, W. Wei, S. Pi et al., "Competitive adsorption of heavy metals by extracellular polymeric substances extracted from Klebsiella sp. J1," *Bioresource Technology*, vol. 196, pp. 533–539, 2015.

[34] A. Li, C. Zhou, Z. Liu et al., "Direct solid-state evidence of H_2-induced partial U(VI) reduction concomitant with adsorption by extracellular polymeric substances (EPS)," *Biotechnology and Bioengineering*, vol. 115, no. 7, pp. 1685–1693, 2018.

[35] W. Wei, A. Li, F. Ma et al., "Simultaneous sorption and reduction of Cr(VI) in aquatic system by microbial extracellular polymeric substances from Klebsiella sp. J1," *Journal of Chemical Technology & Biotechnology*, vol. 93, no. 11, pp. 3152–3159, 2018.

[36] W. Wei, A. Li, J. Yang et al., "Synergetic effects and flocculation behavior of anionic polyacrylamide and extracellular polymeric substrates extracted from Klebsiella sp. J1 on improving soluble cadmium removal," *Bioresource Technology*, vol. 175, pp. 34–41, 2015.

[37] S. Pi, A. Li, W. Wei et al., "Synthesis of a novel magnetic nanoscale biosorbent using extracellular polymeric substances from Klebsiella sp. J1 for tetracycline adsorption," *Bioresource Technology*, vol. 245, no. Part A, pp. 471–476, 2017.

[38] W. Wei, A. Li, S. Pi et al., "Synthesis of core–shell magnetic nanocomposite Fe_3O_4@ microbial extracellular polymeric substances for simultaneous redox sorption and recovery of silver ions as silver nanoparticles," *ACS Sustainable Chemistry & Engineering*, vol. 6, no. 1, pp. 749–756, 2017.

[39] S. Ghorai, A. Sinhamahpatra, A. Sarkar, A. B. Panda, and S. Pal, "Novel biodegradable nanocomposite based on XG-g-PAM/SiO_2: application of an efficient adsorbent for Pb^{2+} ions from aqueous solution," *Bioresource Technology*, vol. 119, pp. 181–190, 2012.

[40] A. Çabuk, T. Akar, S. Tunali, and S. Gedikli, "Biosorption of Pb(II) by industrial strain of Saccharomyces cerevisiae immobilized on the biomatrix of cone biomass of Pinus nigra: equilibrium and mechanism analysis," *Chemical Engineering Journal*, vol. 131, no. 1-3, pp. 293–300, 2007.

[41] Y. A. Aydın and N. D. Aksoy, "Adsorption of chromium on chitosan: optimization, kinetics and thermodynamics," *Chemical Engineering Journal*, vol. 151, no. 1-3, pp. 188–194, 2009.

[42] S. Chakravarty, A. Mohanty, T. N. Sudha et al., "Removal of Pb(II) ions from aqueous solution by adsorption using bael leaves (Aegle marmelos)," *Journal of Hazardous Materials*, vol. 173, no. 1-3, pp. 502–509, 2010.

[43] S. Pi, A. Li, D. Cui et al., "Biosorption behavior and mechanism of sulfonamide antibiotics in aqueous solution on extracellular polymeric substances extracted from Klebsiella sp. J1," *Bioresource Technology*, vol. 272, pp. 346–350, 2019.

[44] J. Yang, D. Wu, A. Li et al., "The addition of N-hexanoyl-homoserine lactone to improve the microbial flocculant production of Agrobacterium tumefaciens strain F2, an exopolysaccharide bioflocculant-producing bacterium," *Applied Biochemistry and Biotechnology*, vol. 179, no. 5, pp. 728–739, 2016.

[45] L. Zhou, A. Li, F. Ma et al., "Combining high electron transfer efficiency and oxidation resistance in nZVI with coatings of microbial extracellular polymeric substances to enhance Sb(V) reduction and adsorption," *Chemical Engineering Journal*, vol. 395, p. 125168, 2020.

[46] C. Y. Lai, Q. Y. Dong, J. X. Chen et al., "Role of extracellular polymeric substances in a methane based membrane biofilm reactor reducing vanadate," *Environmental Science & Technology*, vol. 52, no. 18, pp. 10680–10688, 2018.

[47] P. L. Lv, L. D. Shi, Q. Y. Dong, B. Rittmann, and H. P. Zhao, "How nitrate affects perchlorate reduction in a methane-based biofilm batch reactor," *Water Research*, vol. 171, p. 115397, 2020.